Nano Research 2017, 10(3): 933–940
DOI 10.1007/s12274-016-1352-y
Research Article
ISSN 1998-0124
CN 11-5974/O4

On-surface synthesis of covalent coordination polymers on micrometer scale

Mathieu Koudia[1], Elena Nardi[1], Olivier Siri[2] (✉), and Mathieu Abel[1] (✉)

[1] *Aix Marseille Université, CNRS, IM2NP UMR 7334, 13397, Marseille, France*
[2] *Aix Marseille Université, CNRS, CINaM UMR 7325, 13288, Marseille, France*

Received: 30 September 2016
Revised: 25 October 2016
Accepted: 28 October 2016

KEYWORDS
on-surface synthesis, scanning tunneling microscopy (STM), two-dimensional polymer, covalent organic frameworks

ABSTRACT

On-surface synthesis under ultrahigh vacuum provides a promising strategy to control matter at the atomic level, with important implications for the design of new two-dimensional materials having remarkable electronic, magnetic, or catalytic properties. This strategy must address the problem of limited extension of the domains due to the irreversible nature of covalent bonds, which prevents the ripening of defects. We show here that extended materials can be produced by a controlled co-deposition process. In particular, co-deposition of quinoid zwitterion molecules with iron atoms on a Ag(111) surface held at 570 K allows the formation of micrometer-sized domains based on covalent coordination bonds. This work opens up the construction of micrometer-scale single-layer covalent coordination materials under vacuum conditions.

1 Introduction

In recent years, the development of two-dimensional (2D) organic materials has become the focus of intense research owing to their unique physical and chemical properties [1–4]. A major challenge in this field is to increase the strength of intermolecular bonds from supramolecular to covalently linked 2D materials. Unlike non-covalent bonds, covalent bonds formed by organic precursors are crucial because they enable single-layer organic networks with unique electronic conduction and robustness [5–10]. In this context, on-surface synthesis has emerged as a remarkable strategy, in which the surface is used as a template to catalyze reactions in two dimensions at solid/liquid interfaces [11–13] or under ultrahigh vacuum (UHV) conditions [14–16]. Although 2D supramolecular metal–organic coordination networks (MOCNs) (i.e., non-covalent bonds) are commonly described [17, 18], covalent interactions between metal and organic molecules were recently used to synthesize covalent metal ligand coordination networks on surfaces [19–22]. The versatility of this bottom-up approach offers an unlimited combination of synthons and metal precursors [23, 24]. Nevertheless, the irreversible nature of covalent bonds negatively affects on-surface synthesis under

Address correspondence to Olivier Siri, olivier.siri@univ-amu.fr; Mathieu Abel, mathieu.abel@im2np.fr

vacuum, leading to a large number of defects and limited spatial extension, which represent a critical technological limit. Different strategies have been employed to overcome these limitations: engineering the ligand design for sequential growth [25–27], modifying the substrate reactivity, or adjusting the deposition conditions [28, 29]. By using these approaches, large networks of size 100 nm could be synthesized under UHV.

In this paper, we report a new strategy based on controlled co-deposition and compare it to sequential deposition, which is commonly employed in on-surface synthesis [19, 30, 31]. Organic molecules and iron atoms are first deposited on Ag(111) and then annealed to activate the reaction. The reaction occurs randomly on the substrate, and polymer domains of limited size are formed. The high nucleation density of polymeric domains under UHV limits the extent of growth because covalent bond formation is irreversible. Finally, to overcome this limitation, we provide a new method that allows selection in the nucleation process, leading to micrometer-scale covalent polymers. Our strategy breaks from precedent by using co-deposition of both species on a substrate held at a temperature above the desorption temperature of the molecules [16]. In this way, the growth of existing domains is favored over the nucleation of new ones. Covalent metal ligand coordination polymers have been formed on the micrometer scale by controlling the growth in the co-polymerization reaction between zwitterionic quinone **1** and iron atoms on a Ag(111) substrate held at 570 K.

2 Results and discussion

First, we carefully select an efficient organic partner that can form covalent metal ligand coordination bonds on surfaces. To this end, key parameters in the ligand design were considered: 1) a low molecular weight to control the sublimation step, 2) delocalization of the π electrons upon covalent metal coordination to form conductive materials, 3) good ability to complex metal centers, affording polynuclear arrays, and 4) a planar structure with unhindered substituents to allow the formation of compact layers on surfaces. In this context, molecule **1** (Scheme 1, where R = H) appeared to be an excellent candidate because of its remarkable structural, electronic, and complexing properties. This compound—which is a rare example of the zwitterion being more stable than its canonical form—was first described in 2002 (R = neopentyl group) [32] and immediately attracted the attention of theoreticians [33–37]. Since then, this class of zwitterions became a reagent of choice in organic chemistry [38], a precursor of bioinhibitors in biochemistry [39], and a building block in surface sciences [40–45]. Importantly, its use as a new ligand in coordination chemistry was investigated and clearly demonstrated its efficiency and versatility in solution, especially in stepwise synthesis leading to covalent coordination complexes of types **2** and **3** (Scheme 1) [46]. In the case of **3**, the reaction proceeds by successive deprotonation/metalation steps from **1**, affording a trinuclear complex in which each quinoid unit is linked to the metal center through two covalent and two coordinative bonds through N and O atoms. As a result, the oxidation state of the metal centers is always +II. Furthermore, the zwitterionic character of the ligand is lost, but its π electrons are still delocalized. Therefore, we anticipated that on-surface synthesis between metal atoms and zwitterion **1** could form extended covalent coordination polymers (Scheme 1) on surfaces as a result of the formation of covalent and coordinative bonds with metals by successive deprotonation/metalation reactions [46]. However, beyond ligand design, the deposition strategy is the key issue in the formation of well-ordered crystalline

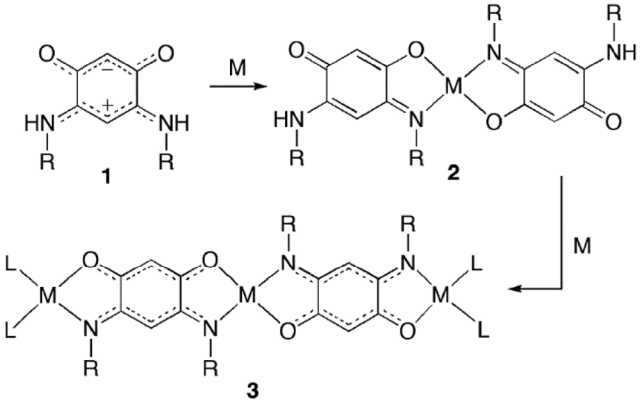

Scheme 1 Chemical structure of 1D covalent coordination polymer. **2** and **3** are obtained from zwitterion **1** and metals M by successive deprotonation reactions (R = neopentyl) [46].

structures on surfaces, which involves a chemical reaction pathway and multiple kinetic processes including nucleation, diffusion of the different species, and desorption or dissolution into the substrate.

2.1 From supramolecular network to covalent coordination polymers

We first investigate the behavior of the selected system in a growth process where molecules of **1** and iron atoms are deposited successively on Ag(111) at room temperature [34]. Annealing the sample at temperatures from 390 to 810 K allows us to study the activation of the on-surface reaction between the two species. The structural arrangement at the atomic level is investigated by scanning tunneling microscopy (STM), and the chemical nature of the bonds (supramolecular or covalent) can influence the direct visualization of the electronic density of states (DOS) [19, 31]. After an initial annealing at 390 K to increase the diffusion length, a well-ordered network is obtained (Fig. 1(a)) that differs from the network obtained with molecules alone Fig. S1 in the Electronic Supplementary Material (ESM) [47]. Triangular domains up to 50 nm in size are formed; they consist of a 2D honeycomb structure with lattice parameters of 14.3 ± 0.5 Å aligned in the close-packed directions of the substrate. These measurements are consistent with density functional theory (DFT) simulations of a supramolecular MOCN of stoichiometry 2:3 (inset, Fig. 1(c)). Each Fe atom interacts with three molecules of **1** in a nearly threefold symmetry, resulting in lattice parameters of 14.3 and 14.5 Å, with 59.8° between them. Annealing this network at 510 K completely changes the shape of the molecular domains from triangular to needle-like (Fig. 1(b)). Small domains (20–30 nm) are observed oriented in six equivalent directions at ±15° from the close-packed directions of the substrate. STM inspection of these domains shows that they are composed of chains of continuous DOS, where bright protrusions and dark sticks alternate with a periodicity of 8.0 ± 0.5 Å (Fig. 1(d)). The image contrasts with an STM image of the MOCN (Fig. 1(c)), in which molecules are distinguished from iron atoms through a discontinuity in the DOS between the different species. These measurements reveal the covalent nature of the bond between the metal and the ligand, which is emphasized

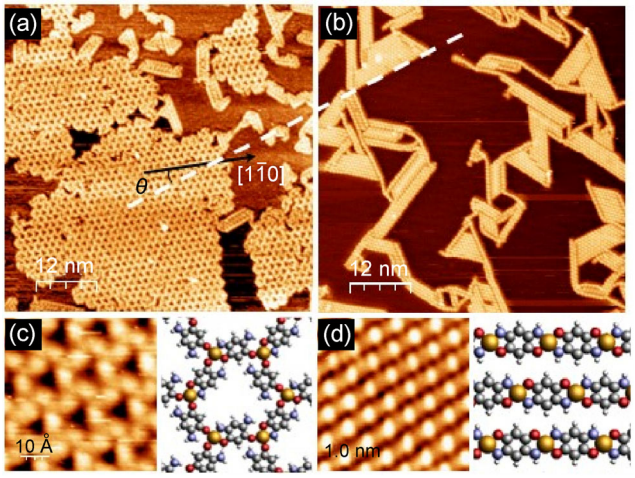

Figure 1 From MOCN to covalent polymers. STM images of the structural domains of zwitterion molecules and iron atoms deposited successively on Ag(111) at room temperature and annealed at ((a) and (c)) 390 and ((b) and (d)) 510 K. Insets show associated DFT models without substrate. C, N, O, H, and Fe are represented as gray, blue, red, white, and orange spheres, respectively. Images are ((a) and (b)) 80 nm × 80 nm and ((c) and (d)) 5 nm × 5 nm.

by the symmetry modification between the MOCN and the needle-like domains obtained after annealing at 390 and 510 K, respectively. The evolution of the nitrogen environment, from amino groups (molecules alone and MOCN) to covalent bonds with Fe atoms (needle-like domains), is confirmed by X-ray photoelectron spectroscopy (XPS) measurements of the N 1s core-level binding energy (Fig. S2 in the ESM). On molecule **1**, the N 1s binding energy is measured as 399.4 eV, which is comparable with that of nitrogen atoms in amino groups [48]. This binding energy then shifts to 397.8 eV for covalent polymers (Fig. S2(a) in the ESM), which is comparable with that of nitrogen atoms bonded covalently to metal in metallophthalocyanine [49]. Importantly, the N 1s spectrum of MOCN is very similar to that of the molecule alone (Fig. S2(b) in the ESM), confirming that deprotonation occurs only for covalent interactions. DFT calculations show that a linear structure of alternating metals and molecules in its pristine form (with all hydrogen atoms) is possible but costs 1.1 eV per Fe atom compared to the threefold complex. It is unlikely that these linear domains appear with increasing temperature. Rather, they appear from the known deprotonation reaction described in Scheme 1, which allows a 0.68 eV

gain in energy per Fe atom, compared to the non-dehydrogenated linear complex (Figs. S3–S5 in the ESM). Furthermore, this evolution from threefold to linear symmetry already occurs at room temperature: 6 days after the elaboration, threefold symmetry domains are completely reorganized in linear arrangements (Fig. S6 in the ESM). The linear experimental polymer is consistent with DFT simulations of a dehydrogenated polymer line (inset, Fig. 1(d)). These lines are organized, and a quasi-hexagonal network with lattice parameters of 7.7 and 7.8 Å is found that comprises Fe atoms bound to the deprotonated form of molecule **1**. The covalent coordination lines are then stacked together to form a 2D self-assembly domain bound by multipolar electrostatic interchain interactions. Increasing the annealing temperature to 690 K allows their diffusion: The weak interchain interactions are broken, and the lines are dispersed on the surface (Fig. S7 in the ESM). Finally, the polymer is completely degraded at 810 K. On the basis of the previously mentioned complexing properties of **1**, the DOS measurements, and the extreme temperature resilience of the chains, we unambiguously prove the covalent nature of the bond between the metal and the ligand from the reported deprotonation of **1** (as observed in solution; see Scheme 1). Moderate annealing at 510 K allows the formation of polymeric domains aligned along six equivalent directions with a random nucleation density of one domain per 100 nm^2. Furthermore, the irreversible nature of covalent bond formation is responsible for a large number of defects that cannot be healed or removed by annealing [28, 29]. At this stage, the random nucleation process and the steric hindrance between domains limit the extent of the covalent polymer. It therefore appears necessary to control the nucleation to 1) select a limited number of germs and 2) promote the growth of existing nuclei at the expense of new nucleation. This is a well-known issue in studies of the classical phase transition, which has not yet been achieved in on-surface synthesis under UHV [50].

2.2 Controlling nucleation and growth process: toward micrometer-scale covalent coordination polymers

The nucleation and growth process can be tuned by controlling the deposition of the species on the Ag(111) substrate. To this end, our strategy consists of co-deposition of molecules and metal atoms on a substrate maintained at a temperature above the desorption temperature of the molecules alone, which is estimated to be 420 K. As a result, the only molecules remaining on the surface are those that found an iron atom to bind to; the rest are desorbed. Figure 2 shows clearly the efficiency of this new approach. The initial state of nucleation is studied for three Fe effective fluxes, 0.4×10^{12}, 1.6×10^{12}, and 4.5×10^{12} iron atoms·cm^{-2}·min^{-1}, with a constant molecular flux (0.05 ML·min^{-1}) and substrate temperature. A substrate temperature of 570 K is chosen to provide a good balance between diffusion and reaction, as detailed below.

For the lowest flux (Fig. 2(a)), a small quantity of iron atoms is deposited in 40 min, producing a few domains of short covalent chains on the surface. Increasing the Fe flux (Figs. 2(b) and 2(c)) results in a progressive increase in the length of the linear covalent chains. In all cases, the covalent metal ligand coordination polymers measured by STM and XPS correspond to one molecule per iron atom, whereas the number of Fe atoms increases from 16×10^{12} iron atoms·cm^{-2} to 90×10^{12} iron atoms·cm^{-2}. Moreover, 80% of the domains are aligned 15° from the close-packed direction of the substrate. In addition, step edges are reorganized in facets aligned with the Ag(111) close-

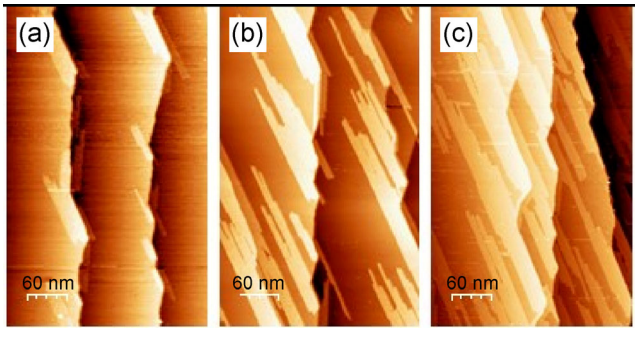

Figure 2 Controlling the nucleation of the polymeric domain. STM images (300 nm × 475 nm) showing the effect of the iron deposition rate on the extent of the crystalline chains of zwitterion molecules and iron atoms co-deposited on Ag(111) held at 570 K. Effective fluxes and deposition times are (a) 0.4×10^{12} Fe atoms·cm^{-2}·min^{-1} for 40 min, resulting in 10% surface coverage, (b) 1.6×10^{12} Fe atoms·cm^{-2}·min^{-1} for 40 min, resulting in 30% surface coverage, and (c) 4.5×10^{12} iron atoms·cm^{-2}·min^{-1} for 20 min, resulting in 50% surface coverage.

packed direction, resulting in a 45° angle between the polymeric domains and the faceted step edges, as shown in Fig. 2. STM measurements of the nucleation density are one domain per 1.3 × 10^4 nm², one domain per 10^4 nm², and one domain per 0.5 × 10^4 nm², respectively, indicating only minor changes among the three fluxes. At the same time, the length of the linear chains and the coverage increase with the quantity of Fe atoms: from 80 nm to 200 and 600 nm long, and from 9% to 33% and 50%, respectively.

Compared to the first sequential growth method presented above, which uses annealing of the deposited materials, the co-deposition method dramatically enhances the growth process, reducing the nucleation density by a factor 200. Furthermore, the interaction of the chains with the step edges makes it possible to select the domain orientation to avoid the appearance of six equivalent directions and promote growth in only one preferred direction at the expense of new nucleation. These results clearly demonstrate the efficiency of the method, which consists of co-deposition of molecules and metals on a substrate maintained at a temperature above the desorption temperature of the molecules. The substrate temperatures during co-deposition determine the kinetics of the reaction. Co-deposition at different substrate temperatures (390–630 K) is investigated for constant molecular and iron fluxes of 0.05 ML·min^{-1} and 4.5 × 10^{12} iron atoms·cm^{-2}·min^{-1}, respectively (Fig. 3). Co-deposition at 390 K (below the desorption temperature of the molecules) leads to the formation of triangular domains up to 50 nm in size consisting of a 2D honeycomb network with a lattice parameter of 14.3 Å aligned with the close-packed directions of the substrate, similar to the MOCN observed after 390 K annealing of the species (Fig. 1(a)).

Increasing the substrate temperature to 510 and 570 K allows the formation of covalent chains comparable to the needle-like domains obtained previously. Then, disordered lines are observed at 630 K (Fig. 3). For co-deposition at 510 K, the lines are aligned along six equivalent directions at ±15° from the close-packed directions of the substrate, and the domain length reaches 200 nm. Nucleation of domains at step edges and terraces leads to the formation of domains in six equivalent directions, preventing their extension

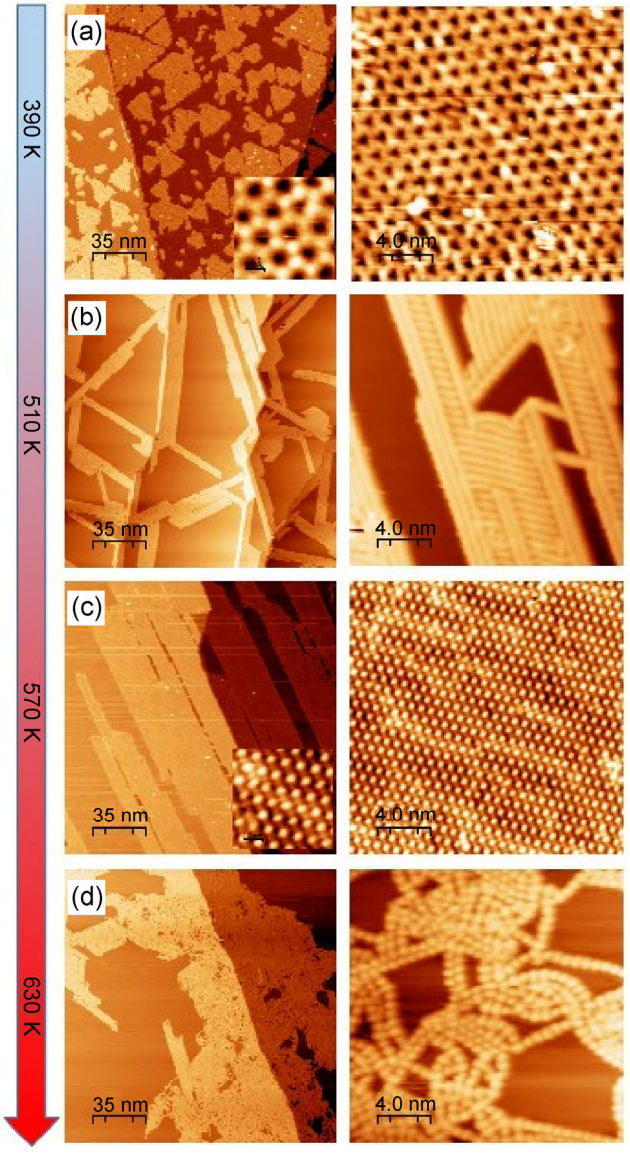

Figure 3 Effect of the substrate temperature during co-deposition of molecules of **1** and Fe atoms on Ag(111) maintained at a temperature between 390 and 630 K. Molecular and Fe fluxes are 0.5 ML·min^{-1} and 4.5 × 10^{12} iron atoms·cm^{-2}·min^{-1}, respectively. Deposition time is 20 min. STM images on the left are 175 nm × 175 nm, with 5 nm × 5 nm insets. Images on the right are 20 nm × 20 nm.

because of steric hindrance. It is only when co-deposition is performed at 570 K that the domains extend up to 600 nm because nucleation occurs only at step edges and no longer occurs on the terraces. At this stage, the length limitation comes from the width of the terraces and the orientation of the steps with respect to that of the needles (Figs. S8 and S9 in the ESM). Finally, the needles can extend freely over the

micrometer range when the step edges are aligned with the preferential growth direction of the polymeric domains.

3 Conclusion

Covalent coordination polymers were formed under UHV by on-surface synthesis between zwitterionic quinone **1** and iron atoms successively deposited on Ag(111), after thermal activation of the reaction. As the reaction occurs randomly, small polymeric domains oriented in six equivalent directions are formed. We demonstrate that co-deposition above the desorption temperature of a component makes it possible to reduce the nucleation density and control the growth. This method enables a dramatic decrease in the quantity of defects usually observed in on-surface synthesis owing to the irreversible nature of covalent bond formation under UHV. Importantly, unprecedented micrometer-scale covalent coordination polymers are now attainable with this strategy. Our approach paves the way to many other organic/inorganic covalent materials having sufficient size to be transferred or isolated for further measurements or functionalization.

Electronic Supplementary Material: Supplementary material (XPS measurements, computational and experimental methods and supplementary STM images) is available in the online version of this article at http://dx.doi.org/10.1007/s12274-016-1352-y.

References

[1] Barth, J. V. Molecular architectonic on metal surfaces. *Annu. Rev. Phys. Chem.* **2007**, *58*, 375–407.

[2] Elemans, J. A. A. W.; Lei, S. B.; De Feyter, S. Molecular and supramolecular networks on surfaces: From two-dimensional crystal engineering to reactivity. *Angew. Chem., Int. Ed.* **2009**, *48*, 7298–7332.

[3] Kudernac, T.; Lei, S. B.; Elemans, J. A. A. W.; De Feyter, S. Two-dimensional supramolecular self-assembly: Nanoporous networks on surfaces. *Chem. Soc. Rev.* **2009**, *38*, 402–421.

[4] Zhuang, X. D.; Mai, Y. Y.; Wu, D. Q.; Zhang, F.; Feng, X. L. Two-dimensional soft nanomaterials: A fascinating world of materials. *Adv. Mater.* **2015**, *27*, 403–427.

[5] Cai, J. M.; Ruffieux, P.; Jaafar, R.; Bieri, M.; Braun, T.; Blankenburg, S.; Muoth, M.; Seitsonen, A. P.; Saleh, M.; Feng, X. L. et al. Atomically precise bottom-up fabrication of graphene nanoribbons. *Nature* **2010**, *466*, 470–473.

[6] Grill, L.; Dyer, M.; Lafferentz, L.; Persson, M.; Peters, M. V.; Hecht, S. Nano-architectures by covalent assembly of molecular building blocks. *Nat. Nanotechnol.* **2007**, *2*, 687–691.

[7] Krasnikov, S. A.; Doyle, C. M.; Sergeeva, N. N.; Preobrajenski, A. B.; Vinogradov, N. A.; Sergeeva, Y. N.; Zakharov, A. A.; Senge, M. O.; Cafolla, A. A. Formation of extended covalently bonded Ni porphyrin networks on the Au(111) surface. *Nano Res.* **2011**, *4*, 376–384.

[8] Shchyrba, A.; Wäckerlin, C.; Nowakowski, J.; Nowakowska, S.; Björk, J.; Fatayer, S.; Girovsky, J.; Nijs, T.; Martens, S. C.; Kleibert, A. et al. Controlling the dimensionality of on-surface coordination polymers via endo- or exoligation. *J. Am. Chem. Soc.* **2014**, *136*, 9355–9363.

[9] Vasseur, G.; Fagot-Revurat, Y.; Sicot, M.; Kierren, B.; Moreau, L.; Malterre, D.; Cardenas, L.; Galeotti, G.; Lipton-Duffin, J.; Rosei, F. et al. Quasi one-dimensional band dispersion and surface metallization in long-range ordered polymeric wires. *Nat. Commun.* **2016**, *7*, 10235.

[10] Zhang, Y. Q.; Kepčija, N.; Kleinschrodt, M.; Diller, K.; Fischer, S.; Papageorgiou, A. C.; Allegretti, F.; Björk, J.; Klyatskaya, S.; Klappenberger, F. et al. Homo-coupling of terminal alkynes on a noble metal surface. *Nat. Commun.* **2012**, *3*, 1286.

[11] Guan, C. Z.; Wang, D.; Wan, L. J. Construction and repair of highly ordered 2D covalent networks by chemical equilibrium regulation. *Chem. Commun.* **2012**, *48*, 2943–2945.

[12] Dienstmaier, J. F.; Medina, D. D.; Dogru, M.; Knochel, P.; Bein, T.; Heckl, W. M.; Lackinger, M. Isoreticular two-dimensional covalent organic frameworks synthesized by on-surface condensation of diboronic acids. *ACS Nano* **2012**, *6*, 7234–7242.

[13] Yu, Y. X.; Lin, J. B.; Wang, Y.; Zeng, Q. D.; Lei, S. B. Room temperature on-surface synthesis of two-dimensional imine polymers at the solid/liquid interface: Concentration takes control. *Chem. Commun.* **2016**, *52*, 6609–6612.

[14] Clair, S.; Abel, M.; Porte, L. Growth of boronic acid based two-dimensional covalent networks on a metal surface under ultrahigh vacuum. *Chem. Commun.* **2014**, *50*, 9627–9635.

[15] Franc, G.; Gourdon, A. Covalent networks through on-surface chemistry in ultra-high vacuum: State-of-the-art and recent developments. *Phys. Chem. Chem. Phys.* **2011**, *13*, 14283–14292.

[16] Lindner, R.; Kühnle, A. On-surface reactions. *Chemphyschem* **2015**, *16*, 1582–1592.

[17] Messina, P.; Dmitriev, A.; Lin, N.; Spillmann, H.; Abel, M.; Barth, J. V.; Kern, K. Direct observation of chiral metal-organic complexes assembled on a Cu(100) surface. *J. Am. Chem. Soc.* **2002**, *124*, 14000–14001.

[18] Lin, N.; Dmitriev, A.; Weckesser, J.; Barth, J. V.; Kern, K. Real-time single-molecule imaging of the formation and dynamics of coordination compounds. *Angew. Chem., Int. Ed.* **2002**, *41*, 4779–4783.

[19] Giovanelli, L.; Savoyant, A.; Abel, M.; Maccherozzi, F.; Ksari, Y.; Koudia, M.; Hayn, R.; Choueikani, F.; Otero, E.; Ohresser, P. et al. Magnetic coupling and single-ion anisotropy in surface-supported Mn-based metal–organic networks. *J. Phys. Chem. C* **2014**, *118*, 11738–11744.

[20] Kezilebieke, S.; Amokrane, A.; Abel, M.; Bucher, J.-P. Hierarchy of chemical bonding in the synthesis of Fe-phthalocyanine on metal surfaces: A local spectroscopy approach. *J. Phys. Chem. Lett.* **2014**, *5*, 3175–3182.

[21] Kezilebieke, S.; Amokrane, A.; Boero, M.; Clair, S.; Abel, M.; Bucher, J.-P. Steric and electronic selectivity in the synthesis of Fe-1,2,4,5-tetracyanobenzene (TCNB) complexes on Au(111): From topological confinement to bond formation. *Nano Res.* **2014**, *7*, 888–897.

[22] Koudia, M.; Abel, M. Step-by-step on-surface synthesis: From manganese phthalocyanines to their polymeric form. *Chem. Commun.* **2014**, *50*, 8565–8567.

[23] Grumelli, D.; Wurster, B.; Stepanow, S.; Kern, K. Bio-inspired nanocatalysts for the oxygen reduction reaction. *Nat. Commun.* **2013**, *4*, 2904.

[24] Gutzler, R.; Stepanow, S.; Grumelli, D.; Lingenfelder, M.; Kern, K. Mimicking enzymatic active sites on surfaces for energy conversion chemistry. *Acc. Chem. Res.* **2015**, *48*, 2132–2139.

[25] Adisoejoso, J.; Li, Y.; Liu, J.; Liu, P. N.; Lin, N. Two-dimensional metallo-supramolecular polymerization: Toward size-controlled multi-strand polymers. *J. Am. Chem. Soc.* **2012**, *134*, 18526–18529.

[26] Faury, T.; Clair, S.; Abel, M.; Dumur, F.; Gigmes, D.; Porte, L. Sequential linking to control growth of a surface covalent organic framework. *J. Phys. Chem. C* **2012**, *116*, 4819–4823.

[27] Lafferentz, L.; Eberhardt, V.; Dri, C.; Africh, C.; Comelli, G.; Esch, F.; Hecht, S.; Grill, L. Controlling on-surface polymerization by hierarchical and substrate-directed growth. *Nat. Chem.* **2012**, *4*, 215–220.

[28] Bieri, M.; Nguyen, M. T.; Gröning, O.; Cai, J. M.; Treier, M.; Aït-Mansour, K.; Ruffieux, P.; Pignedoli, C. A.; Passerone, D.; Kastler, M. et al. Two-dimensional polymer formation on surfaces: Insight into the roles of precursor mobility and reactivity. *J. Am. Chem. Soc.* **2010**, *132*, 16669–16676.

[29] Ourdjini, O.; Pawlak, R.; Abel, M.; Clair, S.; Chen, L.; Bergeon, N.; Sassi, M.; Oison, V.; Debierre, J. M.; Coratger, R. et al. Substrate-mediated ordering and defect analysis of a surface covalent organic framework. *Phys. Rev. B* **2011**, *84*, 125421.

[30] Nardi, E.; Chen, L.; Clair, S.; Koudia, M.; Giovanelli, L.; Feng, X. L.; Müllen, K.; Abel, M. On-surface reaction between tetracarbonitrile-functionalized molecules and copper atoms. *J. Phys. Chem. C* **2014**, *118*, 27549–27553.

[31] Piantek, M.; Serrate, D.; Moro-Lagares, M.; Algarabel, P.; Pascual, J. I.; Ibarra, M. R. Manganese phthalocyanine derivatives synthesized by on-surface cyclotetramerization. *J. Phys. Chem. C* **2014**, *118*, 17895–17899.

[32] Siri, O.; Braunstein, P. Unprecedented zwitterion in quinonoid chemistry. *Chem. Commun.* **2002**, 208–209.

[33] Braunstein, P.; Siri, O.; Taquet, J. P.; Rohmer, M. M.; Bénard, M.; Welter, R. A 6π+6π potentially antiaromatic zwitterion preferred to a quinoidal structure: Its reactivity toward organic and inorganic reagents. *J. Am. Chem. Soc.* **2003**, *125*, 12246–12256.

[34] Delaere, D.; Nam, P. C.; Nguyen, M. T. Electronic structure of zwitterionic diamino-meta-quinonoid molecules: Identity of UV absorption bands. *Chem. Phys. Lett.* **2003**, *382*, 349–354.

[35] Haas, Y.; Zilberg, S. Charge separation in ground-state 1,2,4,5-tetra-substituted benzene derivatives. *J. Am. Chem. Soc.* **2004**, *126*, 8991–8998.

[36] Le, H. T.; Nam, P. C.; Dao, V. L.; Veszprémi, T.; Nguyen, M. T. Molecular and electronic structure of zwitterionic diamino-meta-quinonoid molecules. *Mol. Phys.* **2003**, *101*, 2347–2355.

[37] Sawicka, A.; Skurski, P.; Simons, J. An excess electron binding to the "purple" zwitterion quinonoid. *Chem. Phys. Lett.* **2002**, *362*, 527–533.

[38] Braunstein, P.; Siri, O.; Taquet, J. P.; Yang, Q. Z. Regioselective carbon–carbon bond formation reactions between TCNE or TCNQ and a quinonoid ring. *Angew. Chem., Int. Ed.* **2006**, *45*, 1393–1397.

[39] Braunstein, P.; Siri, O.; Taquet, J. P.; Yang, Q. Z. Toward a 6π+6π zwitterion or a bioinhibitors-related OH-substituted aminoquinone: Identification of a key intermediate in their pH controlled synthesis. *Chem.—Eur. J.* **2004**, *10*, 3817–3821.

[40] Fang, Y.; Nguyen, P.; Ivasenko, O.; Aviles, M. P.; Kebede, E.; Askari, M. S.; Ottenwaelder, X.; Ziener, U.; Siri, O.; Cuccia, L. A. Charge-assisted hydrogen bond-directed self-assembly of an amphiphilic zwitterionic quinonemonoimine at the liquid–solid interface. *Chem. Commun.* **2011**, *47*, 11255–11257.

[41] Kunkel, D. A.; Hooper, J.; Simpson, S.; Miller, D. P.; Routaboul, L.; Braunstein, P.; Doudin, B.; Beniwal, S.;

Dowben, P.; Skomski, R. et al. Self-assembly of strongly dipolar molecules on metal surfaces. *J. Chem. Phys.* **2015**, *142*, 101921.

[42] Kunkel, D. A.; Simpson, S.; Nitz, J.; Rojas, G. A.; Zurek, E.; Routaboul, L.; Doudin, B.; Braunstein, P.; Dowben, P. A.; Enders, A. Dipole driven bonding schemes of quinonoid zwitterions on surfaces. *Chem. Commun.* **2012**, *48*, 7143–7145.

[43] Routaboul, L.; Braunstein, P.; Xiao, J.; Zhang, Z. Z.; Dowben, P. A.; Dalmas, G.; Da Costa, V.; Félix, O.; Decher, G.; Rosa, L. G. et al. Altering the static dipole on surfaces through chemistry: Molecular films of zwitterionic quinonoids. *J. Am. Chem. Soc.* **2012**, *134*, 8494–8506.

[44] Simpson, S.; Kunkel, D. A.; Hooper, J.; Nitz, J.; Dowben, P. A.; Routaboul, L.; Braunstein, P.; Doudin, B.; Enders, A.; Zurek, E. Coverage-dependent interactions at the organics–metal interface: Quinonoid zwitterions on Au(111). *J. Phys. Chem. C* **2013**, *117*, 16406–16415.

[45] Yuan, M. H.; Tanabe, I.; Bernard-Schaaf, J.-M.; Shi, Q.-Y.; Schlegel, V.; Schurhammer, R.; Dowben, P. A.; Doudin, B.; Routaboul, L.; Braunstein, P. Influence of steric hindrance on the molecular packing and the anchoring of quinonoid zwitterions on gold surfaces. *New J. Chem.* **2016**, *40*, 5782–5796.

[46] Taquet, J. P.; Siri, O.; Braunstein, P.; Welter, R. Stepwise synthesis, structures, and reactivity of mono-, di-, and trimetallic metal complexes with a 6π+6π quinonoid zwitterion. *Inorg. Chem.* **2004**, *43*, 6944–6953.

[47] Dowben, P. A.; Kunkel, D. A.; Enders, A.; Rosa, L. G.; Routaboul, L.; Doudin, B.; Braunstein, P. The dipole mediated surface chemistry of p-benzoquinonemonoimine zwitterions. *Top. Catal.* **2013**, *56*, 1096–1103.

[48] Lin, Y. P.; Ourdjini, O.; Giovanelli, L.; Clair, S.; Faury, T.; Ksari, Y.; Themlin, J. M.; Porte, L.; Abel, M. Self-assembled melamine monolayer on Cu(111). *J. Phys. Chem. C* **2013**, *117*, 9895–9902.

[49] Bai, Y.; Buchner, F.; Wendahl, M. T.; Kellner, I.; Bayer, A.; Steinrück, H. P.; Marbach, H.; Gottfried, J. M. Direct metalation of a phthalocyanine monolayer on Ag(111) with coadsorbed iron atoms. *J. Phys. Chem. C* **2008**, *112*, 6087–6092.

[50] Christian, J. W. *The Theory of Transformations in Metals and Alloys*; Pergamon: Oxford, UK, 2002.